Thromboinflammation in high-risk human populations

Yuan, L.

CHAPTER 5

Heparan sulfate mimetic fucoidan restores the endothelial glycocalyx and protects against dysfunction induced by serum of COVID-19 patients in the intensive care unit

Lushun Yuan[1], Shuzhen Cheng[2], Wendy M.P.J. Sol[1], Anouk I.M. van der Velden[1], Hans Vink[3,4], Ton J. Rabelink[1], Bernard M. van den Berg[1], in collaboration with the BEAT-COVID study group[5]

The Einthoven Laboratory for Vascular and Regenerative Medicine, department of Internal Medicine, Nephrology[1] and Thrombosis and Hemostasis[2], Leiden University Medical Center, Leiden, the Netherlands.

[3]Department of Physiology, Cardiovascular Research Institute Maastricht, Maastricht, the Netherlands

[4]MicroVascular Health Solutions LLC, Alpine, Utah, USA

[5]BEAT-COVID study group

ERJ Open Res. 2022 May 3;8(2):00652-2021

Abstract

Accumulating evidence proves that endothelial dysfunction is involved in COVID-19 progression. We previously demonstrated that the endothelial surface glycocalyx has a critical role in maintenance of vascular integrity. Here we hypothesized that serum factors of severe COVID-19 patients affect the glycocalyx and result into endothelial dysfunction.

We included blood samples of 32 COVID-19 hospitalized patients at the Leiden University Medical Center: of which 26 from intensive care unit (ICU), 6 non-ICU, 18 convalescent samples 6 weeks after hospital discharge, and of 12 age-matched healthy donors (control) during the first period of the outbreak. First, we determined endothelial (angiopoietin 2, ANG2) and glycocalyx degradation (soluble thrombomodulin, sTM and syndecan-1, sSDC1) markers in plasma.

In plasma of COVID-19 patients, circulating ANG2 and sTM were elevated in patients on the ICU. Primary lung microvascular endothelial cells (HPMEC) and human glomerular microvascular ECs (GEnCs) cultures in the presence of these sera led to EC glycocalyx degradation, barrier disruption, inflammation and increased coagulation on the endothelial surface, significantly different compared to healthy control and non-ICU patient sera. These changes all could be restored in the presence of fucoidan.

In conclusion, our data highlight the link between endothelial glycocalyx degradation, barrier failure and induction of a procoagulant surface in COVID-19 patients on ICU which could be targeted earlier in disease by the presence of heparan sulfate (HS) mimetics.

Keywords: SARS-CoV-2 disease, COVID-19, endothelial dysfunction, glycocalyx, endothelial barrier, coagulation, fucoidan

Introduction

The coronavirus disease 2019 (COVID-19) caused by severe acute respiratory syndrome coronavirus-2 (SARS-CoV-2) has rapidly spread worldwide that lead to an unprecedented global pandemic since late 2019 [1]. Most of the COVID-19 cases are asymptomatic or cause only mild illness [2]. However, in a considerable proportion of patients, respiratory illness that require hospitalization occurred, which might develop into progressive disease and lead to hypoxemic respiratory failure, requiring long-term ventilatory support [3, 4]. Besides severe respiratory symptoms during hospitalization at the intensive care unit (ICU), a high incidence of thromboembolism events was observed [5]. Acute respiratory distress syndrome and coagulopathy are leading causes of COVID-19 patient mortality [6], while endothelial dysfunction is reported to be involved in both acute respiratory distress syndrome (ARDS) and coagulopathy [7, 8]. Consistent with autopsy findings that severe lung endothelial injury was observed in patients who succumbed to COVID-19 [9], COVID-19 could be considered as a vascular disease and vascular dysfunction might play a critical role in the pathogenesis of ARDS and coagulopathy.

The glycocalyx is a key regulator of endothelial cell integrity and homeostasis, it regulates vascular barrier permeability, prevents inflammation and ensures vessel patency [10-13]. It's a gel-like layer composed of the glycosaminoglycans heparan sulfate, hyaluronan (HA), chondroitin sulfate, and associated proteins, that covers the luminal surface of vascular endothelial cells [14]. Inflammation-induced glycocalyx degradation can lead to hyperpermeability of blood vessels, vasodilation disorders, microvascular thrombosis and increased leukocyte adhesion [15]. In previous studies, glycocalyx destruction and dysfunction was observed in sepsis, acute kidney injury and ARDS, and was associated with worse patient outcome [15, 16]. Recently, it was reported that the endothelial glycocalyx-degrading enzyme heparanase contributed to vascular leakage and inflammation, and its activity was associated with disease severity in COVID-19 patients [11, 17]. Meanwhile, the MYSTIC study also provided evidence that glycocalyx health, as measured by changes in the perfused boundary region (PBR), was a predictive prognostic

marker for COVID-19 septic patients [18].

Here we test whether preservation of the endothelial glycocalyx might be an effective intervention to improve vascular health. For this, we examined the possible beneficial effects of the heparan sulfate mimetic fucoidan [19], in restoring the endothelial functionality.

Material and methods

For detailed information see supplemental information

BEAT-COVID cohort study population and study design

A prospective observational cohort study was set up, in which patients with PCR-confirmed SARS-CoV-2 infection after hospital admission were recruited from April 2020 until August 2020, before the use of medication such as dexamethasone and vaccines were implemented (supplementary figure S1). Plasma and serum samples were collected from 32 patients, of which 26 were hospitalized in the ICU and 6 in a non-ICU medical floor. In 18 of the 32 included patients, follow-up data was obtained 6 weeks after discharge from the hospital. In addition, samples of 12 age-matched controls were obtained. Patient characteristics are shown in supplementary Table 1. Due to the limited amount of material per sample that could be obtained pooled sera were used in some experiments as indicated. The trial was registered in the Dutch Trial Registry (NL8589). 12 Age-matched healthy donors with a male: female ratio of 2:1, were included after confirmed negative SARS-CoV-2 IgG. Ethical approval was obtained from the Medical Ethical Committee Leiden-Den Haag-Delft (NL73740.058.20).

Circulating markers of endothelial dysfunction and glycocalyx shedding

Plasma samples were used to measure angiopoietin 2 (Ang-2, DANG20, R&D Systems, Abingdon, UK), soluble thrombomodulin (sTM, M850720096, Diaclone, Besançon, France) and soluble syndecan-1 (sSDC1, DY2780, R&D Systems) according to manufacturer's respective protocols.

Endothelial barrier function assay

Endothelial barrier function analysis was performed with impedance-based cell monitoring using the electric cell-substrate impedance sensing system (ECIS Zθ, Applied Biophysics, New York, USA). ECIS plates (96W20idf PET, Applied Biophysics) were pre-treated with 10 mM L-cysteine and coated with 1% gelatine for primary human glomerular microvascular ECs (GEnCs; ACBRI-128, Cell Systems, Kirkland, WA, USA) or without 1% gelatine for primary pulmonary microvascular endothelial cells (HPMECs; PromoCell, Heidelberg, Germany). HPMECs (p5) were seeded at a concentration of 4.5×10^5 cells/well and for GEnCs (p5), the concentration was 3×10^5 cells/well in EGM medium (basal medium MV, C-22220, PromoCell) supplemented with C-39220 (PromoCell) and 1% antibiotics (penicillin/streptomycin, 15070063, Gibco, Paisley, UK) at 37°C and 5% CO_2.

Initial baseline resistance was measured for 2 hours before endothelial cells were seeded into the plate. Multiple frequency/time mode was used for the real-time assessment of the barrier function. Once the stable monolayer was formed, endothelial cells were incubated with 10% serum (healthy (n=12), COVID-19 non-ICU (n=8) and ICU (n=26)) and measured for 20 hours. Afterwards, modelling data Rb which represents barrier function could be generated.

In additional experiments, HPMECs were exposed to 10% healthy serum (n=12), COVID-19 ICU serum (n=26) with or without fucoidan (10 µg/mL, gift from MicroVascular Health

Solutions LLC, Alpine, UT, USA). The natural fucoidan provided (Iso 9000 and GMP certified from Omnipharm, S.A.S, Chambéry, France) was extracted from *Laminaria japonica* as a powder of 91.20% purity and further tested, for instance, on the presence of heavy metals (arsenic, lead, cadmium, mercury) or microbiology parameters (European Pharmacopoeia VIII, Ed 2,6,12: total plate count, yeast, mold, *E. coli, Salmonella spp.*). A 50x times stock solution was prepared by dissolving the appropriate amount of powder in milliQ water and passed through a 0.22µm filter before use.

RNA isolation and RT-PCR

RNA of cultured cells is isolated using RNeasy Mini Kit (74106, Qiagen, Venlo, The Netherlands) according to manufacturer's protocol RT-PCR analysis was conducted using SYBR Select Master Mix (4472908, Applied Biosystems, Landsmeer, The Netherlands) and specific primers as indicated in supplementary table s2. Gene expression was normalized to GAPDH of 5 separate experiments.

Immunoblotting analysis

Western blots were performed from protein extracts of HPMECs [12]. 10% Mini-PROTEAN® TGX™ Protein Gels (4561031, Bio-Rad Laboratories, Veenendaal, The Netherlands) were used for protein size separation and proteins were transferred to PVDF membranes (1704156, Bio-Rad). Membranes were blocked in 5% milk in PBST at room temperature for 1 hour and further incubated with primary antibody rabbit anti-human ICAM1 (4915, Cell Signalling Technology), rabbit anti-human total NF-κB p65 (8242, Cell Signalling Technology), rabbit anti-human phosphor-NF-κB p65 (Ser536) (3033, Cell Signalling Technology) or mouse anti-human GAPDH (MA5-15738, ThermoFisher) overnight at 4°C. Protein was detected using HRP-conjugated antibody (P0447 and P0448,

Dako, Amstelveen, The Netherlands) and Western Lightning Plus-ECL, Enhanced Chemiluminescence Substrate (NEL103001EA, PerkinElmer, Groningen, The Netherlands). Intensity of the bands were analysed using ImageJ software. Relative intensity was determined by levels of GAPDH.

Immunofluorescence of cultured cells

HPMECs (p5) were cultured in 8-well chamber slides (ibiTreat, µ-Slide 8 Well). Confluent monolayers were incubated with 10% pooled serum (healthy control (pooled n = 12), non-ICU (pooled n = 8) and ICU (pooled n = 26) in no FCS medium for 24 hours. Next, cells were fixed with 4% PFA and 0.2% Triton-X100 in HBSS or 4% PFA in HBSS (for HS and LEA staining) for 10 minutes at room temperature, blocked with 3% goat serum in HBSS and incubated with FITC labelled *Lycopersicon esculentum* (LEA-FITC, L0401, Sigma, Houten, The Netherlands), Mouse Anti-Human VE cadherin (55-7H1; BD Biosciences), Mouse Anti-heparan sulfate (10E4, 370255-1, AMSBIO, Abingdon, UK) or Mouse Anti-TM (MA5-11454, ThermoFisher) at 4°C overnight, followed by an appropriate secondary antibody and phalloidin-TRITC (VE-cadherin samples) for 1 hour. Finally, Hoechst 33528 (1/1,000) was added and cells using a LEICA SP8 WLL confocal microscope (Leica, Rijswijk, the Netherlands). Fluorescent images were analysed using Image J software. Quantification is descripted in Supplementary info.

FX activation by extrinsic tenase complex (TF-FVIIa)

Confluent HPMECs were incubated with 10% control (n=12), COVID-19 non-ICU (n=8) and ICU serum (n=26, with or without presence of fucoidan) in no FCS medium for 24 hours. Cell culture supernatants were collected and centrifuged for ELISA assays. Factor VIIa (80 µL, 10 nM, HCVIIA-0031, Haematologic Technologies, Huissen, The Netherlands) was

added and incubated for 15 minutes at 37°C and 5%CO_2. The reaction was initiated by adding factor X (80 µL, 400 nM, HCX-0050, Haematologic Technologies) to detect the production of active factor X. Aliquots were quenched in HBS supplemented with 50mM EDTA to stop the reaction and determined by SpecXa conversion (250 µM), at 405 nm.

Thrombin generation Assay

Confluent HPMECs were incubated with 10% healthy (n=12), COVID-19 non-ICU (n=8) and ICU serum (n=26, with or without presence of fucoidan) in no FCS medium for 24 hours. Thrombin generation curves were obtained by supplementing normal pooled plasma. Thrombin formation was initiated by adding substrate buffer (FluCa-kit, 86197, Thrombinoscope BV, Leiden, The Netherlands) to the plasma. Thrombin formation was determined using Thrombinoscope software.

Markers of endothelial dysfunction and glycocalyx shedding in cell cultured supernatant

Supernatants collected were used to measure Ang-2, sTM, IL-6 (M9316, Sanquin, Amsterdam, The Netherlands) and VWF (A0082, Dako).

Statistics

Data are presented as mean ± SD, unless indicated otherwise. For all experiments, 3 to 5 independent experiments were performed. Shapiro-Wilk test and Levene test were performed to evaluate the normality and variances first. Then non-paired/paired 2-tailed t test were used to assess the differences between two groups. One-way ANOVA followed by Tukey's multiple comparisons test and Kruskal-Wallis test followed by Dunn's multiple comparisons test were assessed for multiple groups. Statistical analysis were performed

using SPSS statistical software version 25 (SPSS Inc., Chicago, IL) and GraphPad Prism version 8 (Graphpad Inc., La Jolla, CA, USA). A significance level of 0.05 was considered statistically significant.

Results

COVID-19 leads to endothelial dysfunction and glycocalyx degradation

Overall endothelial health in COVID-19 patients was assessed by measuring plasma ANG2 concentrations which were found to be significantly increased in COVID-19 patients on the ICU (figure 1a). ANG2 levels of non-ICU patients were not distinguishable from control levels or recovered patients 6 weeks after discharge. Circulating fragments of thrombomodulin (sTM), one of the glycocalyx components, were also markedly increased in COVID-19 ICU patients compared to healthy controls, non-ICU patients, and after recovery (figure 1b). Shedding of the glycocalyx core protein, syndecan-1 (sSDC1), was found not to be significantly raised in COVID-19 ICU patients in comparison to healthy controls or non-ICU patients (figure 1c). Pearson's correlation between each of 2 markers was analysed and showed that ANG2 moderately correlated with sTM and sSDC1 ($R=0.49$, $p<0.0001$ and $R=0.33$, $p=0.015$ respectively), and sTM positively correlated with sSDC1 ($R=0.50$, $p=0.0002$) indicating that endothelial dysfunction could lead to glycocalyx shedding (figure 1d-f).

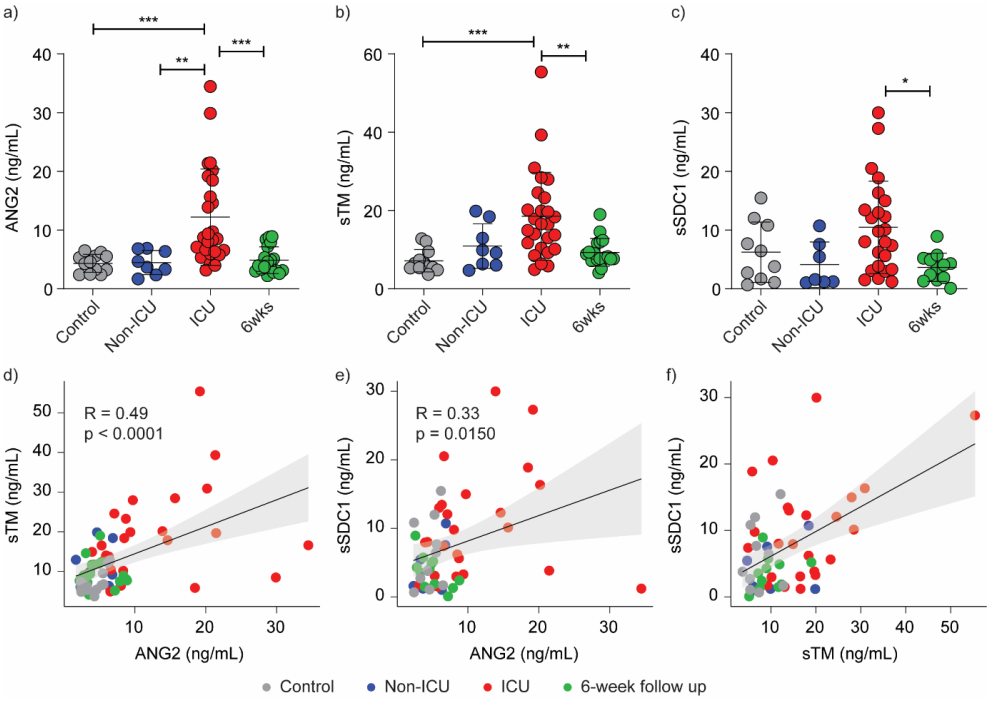

Figure 1 Comparison and association of endothelial dysfunction and glycocalyx shedding related markers in COVID-19 patients and healthy controls. Levels of a) angiopoietin 2 (ANG2), b) soluble thrombomodulin (sTM) and c) soluble syndecan-1 (sSDC1) between healthy controls (grey, n = 12), COVID-19 non-ICU patients (blue, n = 8), COVID-19 ICU patients (red, n = 26) and recovered patients (green, n = 18). Pearson's correlation between d) ANG2 and sTM, e) ANG2 and sSDC1, f) sTM and sSDC1. Graphs represent the mean ± SD. One-way ANOVA followed by Tukey's multiple comparisons test and Pearson's correlation analysis were performed; *p<0.05, **p<0.01, ***p<0.001.

Endothelial glycocalyx degradation in presence of COVID-19 ICU serum

To determine the effect of systemic blood factors during COVID-19 disease on endothelial surface glycocalyx expression, HPMECs were cultured in the presence of 10% pooled serum of either healthy controls, COVID-19 non-ICU and COVID-19 ICU patients for 24 hours and stained for overall glycocalyx presence (LEA-FITC), for heparan sulfates (HS) and thrombomodulin (TM). The COVID-19 ICU group showed a marked reduced surface

expression of LEA-FITC (figure 2a,b), TM (figure 2a,c) and HS (figure S2a,b), compared to healthy control- and COVID-19 non-ICU groups.

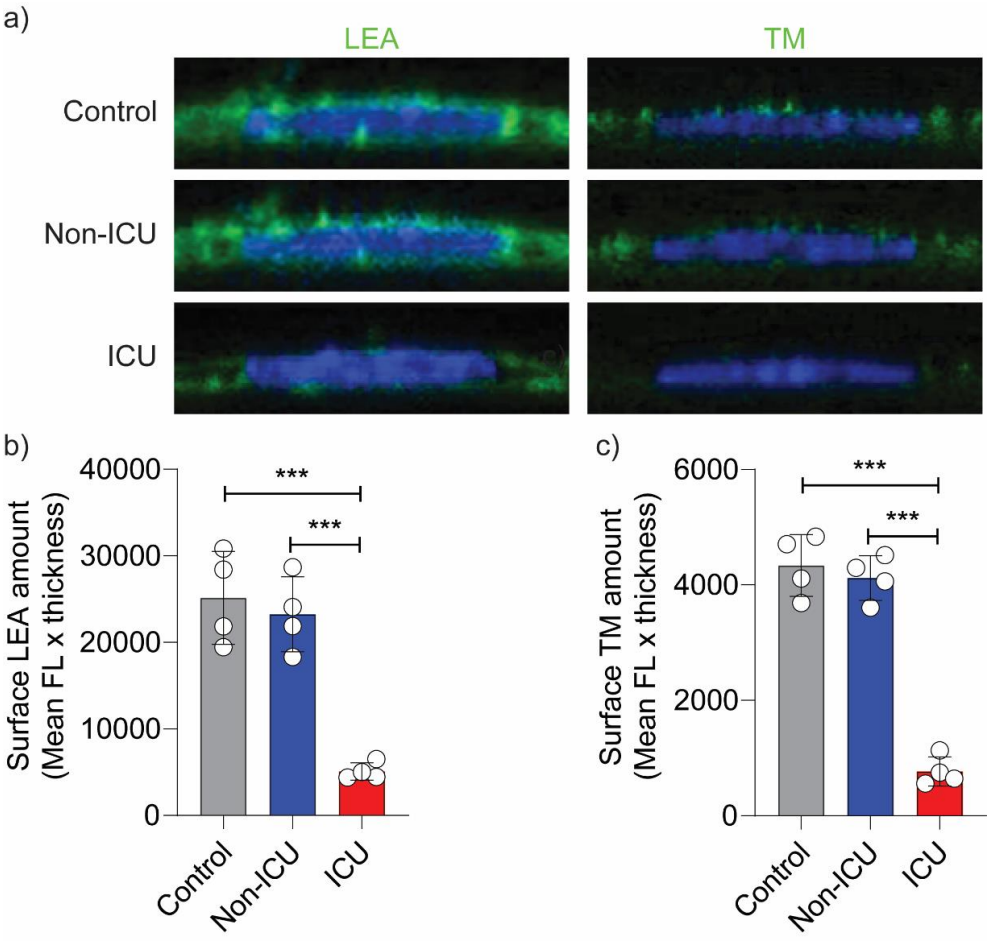

Figure 2 Loss of glycocalyx in primary human pulmonary microvascular endothelial cells in presence of serum of COVID-19 patients on ICU. a) Representative fluorescence confocal images of *Lycopersicon esculentum*-FITC (LEA) or anti-thrombomodulin (TM) staining on the surface of primary human pulmonary microvascular endothelial cells (HPMECs) in the presence of 10% serum of pooled- healthy controls (n = 12), COVID-19 non-ICU (n = 8) and COVID-19 ICU (n = 26) samples for 24hrs. HPMEC surface expression quantification of b) LEA-FITC and c) TM in the presence of 10% pooled- healthy control , COVID-19 non-ICU and COVID-19 ICU serum for 24hrs All values are given as mean ± SD of 4 independent experiments. One-way ANOVA followed by Tukey's multiple

comparisons test was performed; ***p<0.001.

COVID-19 ICU serum induced loss of endothelial cell barrier function

Next, the ability of COVID-19 serum to disrupt the barrier integrity of primary human microvascular endothelial cells was tested. In contrast to healthy controls and COVID-19 non-ICU patients, serum from COVID-19 ICU patients induced a reduction in resistance of both HPMECs and GEnCs (figure 3a,c). The calculated areas under curve for the final 15 hours, showed that the COVID-19 ICU samples were significantly below healthy control samples, especially in HPMECs (figure 3b,d). The modelling value for barrier function, Rb, representing cell-cell-contacts, resulted in a similar reduction upon exposure to serum of COVID-19 ICU patients (figure 3e-h). Interestingly, we could find differences in vascular bed susceptibility in response to COVID-19 ICU patient sera, showing that the lung originating HPMECs were more sensitive than the kidney isolated GEnCs. While resistance and barrier function decreased in HPMECs during the entire incubation time, in GEnCs, both factors started to recover after 15 hours (figure 3a,c,e,g). Reduction of VE-cadherin, together with reduced cellular junction area, and increasing stress fibre formation in response to COVID-19 ICU patient serum in comparison to COVID-19 non-ICU and healthy control sera confirmed this EC barrier loss (figure 3i,j). This observed barrier function reduction correlated with the increased plasma levels of ANG2, sTM and sSDC1, linking EC activation and glycocalyx shedding to possible endothelial loss of barrier function in patients (figure 3k).

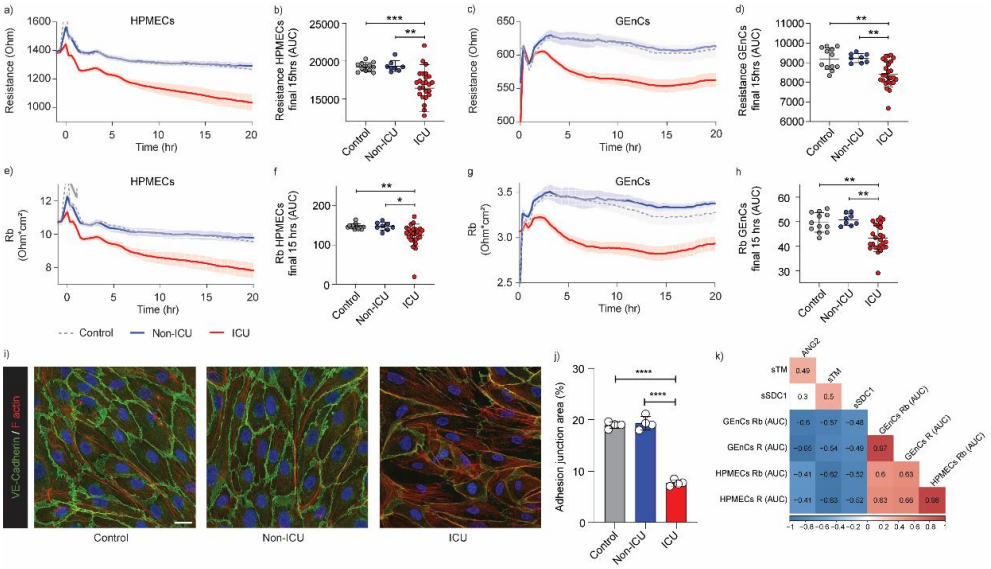

Figure 3 Serum mediators of COVID-19 patients on ICU induce microvascular barrier disruption. Barrier integrity parameter, resistance of a + b) primary human pulmonary microvascular endothelial cells (HPMECs) and c + d) primary human glomerular microvascular ECs (GEnCs) assessed by electric cell-substrate impedance sensing system (ECIS Zθ) in response to stimulation with 10% serum (at t=0hr) of healthy controls (n=12, grey dotted line), COVID-19 non-ICU (n=8, blue line) and COVID-19 ICU (n=26, red line). Cell-cell contact parameter, Rb of e + f) HPMECs and g + h) GEnCs assessed by ECIS Zθ in response to stimulation with 10% serum (at t=0hr) of healthy controls (n=12, grey dotted line), COVID-19 non-ICU (n=8, blue line) and COVID-19 ICU (n=26, red line). In some cases, multiple samples (in ICU and out of ICU) from the same patient at different time points were obtained. Data of raw resistance and Rb values were shown and presented as mean ± SEM. Quantification of barrier integrity was based on the measurements of area under curve over the final 15 hours of b) HPMECs and d) GEnCs. Quantification of cell-cell contact was based on the measurements of area under curve over the final 15 hours of f) HPMECs and h) GEnCs. i) Representative confocal images of VE-cadherin (green) and F-actin (red) staining on HPMECs in the presence of 10% pooled- healthy control (n = 12), COVID-19 non-ICU (n = 8) and COVID-19 ICU (n = 26) serum for 24hrs (scale bar = 20 µm). j) Quantification of adhesion junction percentage of HPMECs in the presence of 10% pooled- healthy control, COVID-19 non-ICU and COVID-19 ICU serum for 24hrs of 4 independent experiments. Graphs represent the mean ± SD. k) Pearson's correlation heatmap between endothelial dysfunction and glycocalyx shedding related markers (angiopoietin 2, soluble thrombomodulin and soluble syndecan-1) and barrier function related parameters (last 15hrs AUC of R and Rb in HPMECs and GEnCs). Colours represent correlation, blue means negative correlation and red means positive correlation. Blank means no significance. One-way ANOVA followed by Tukey's multiple comparisons test

and Kruskal-Wallis test followed by Dunn's multiple comparisons test and were performed; *p<0.05, **p<0.01, ***p<0.001, ****p<0.0001.

Fucoidan restores glycocalyx and ameliorates endothelial cell activation induced by COVID-19 serum

To test whether loss of surface glycocalyx could be restored, we cultured HPMECs in the presence of both ICU patient sera and the HS mimetic fucoidan (10 µg/mL). Supplementation of fucoidan during culture in the presence of ICU serum dramatically restored the glycocalyx as was shown by LEA-FITC staining (figure 4a,b) and TM expression (figure 4a,c).

One of the mechanisms of glycocalyx loss is through enzymatic HS degradation by heparanase (HPSE-1), which is elevated in plasma of COVID-19 patients [17]. In our *in vitro* cultured HPMECs in the presence of 10% pooled patient or healthy control serum we observed significantly induced *HPSE-1* gene expression in cells from the ICU patient group without a change in the non-ICU group (supplementary figure S3a). Mechanistically, we observed that addition of fucoidan showed a trend of decreasing *HPSE-1* gene expression (supplementary figure S3a) in the ICU patient group, which coincided with reduced syndecan-1 gene expression (*SDC1*) and was significantly restored after fucoidan supplementation (supplementary figure S3b).

Further evaluation of endothelial cell dysfunction in the presence of patient sera showed that compared to healthy controls, gene expression of *ANGPT2*, *ICAM-1* and *IL-6* were significantly up regulated in the presence of COVID-19 ICU sera (figure S3c-e), while no effect was found with COVID-19 non-ICU samples. At protein level, ICAM-1 expression was also increased in presence of COVID-19 ICU serum (figure 4d,e). Since endothelial activation could induce NFκB activation, we then detected the NFκB phosphorylation levels and found a marked activation of these factors in ECs in the presence of COVID19 ICU sera, without significant changes between healthy control, COVID-19 non-ICU and

fucoidan supplementation groups (figure 4d,f). This increased endothelial activation was further corroborated by the induced amount of released von Willebrand factor (VWF) and ANG2, from the Weibel-Palade bodies (WPBs) upon activation and secretion of IL-6 and shedding of sTM by these cells (supplementary figure S4). When comparing the response on individual patient serum level, fucoidan reduced these markers significantly (figure 4g-j), in line with the observed normalization of ICAM-1 expression (figure 4d,e).

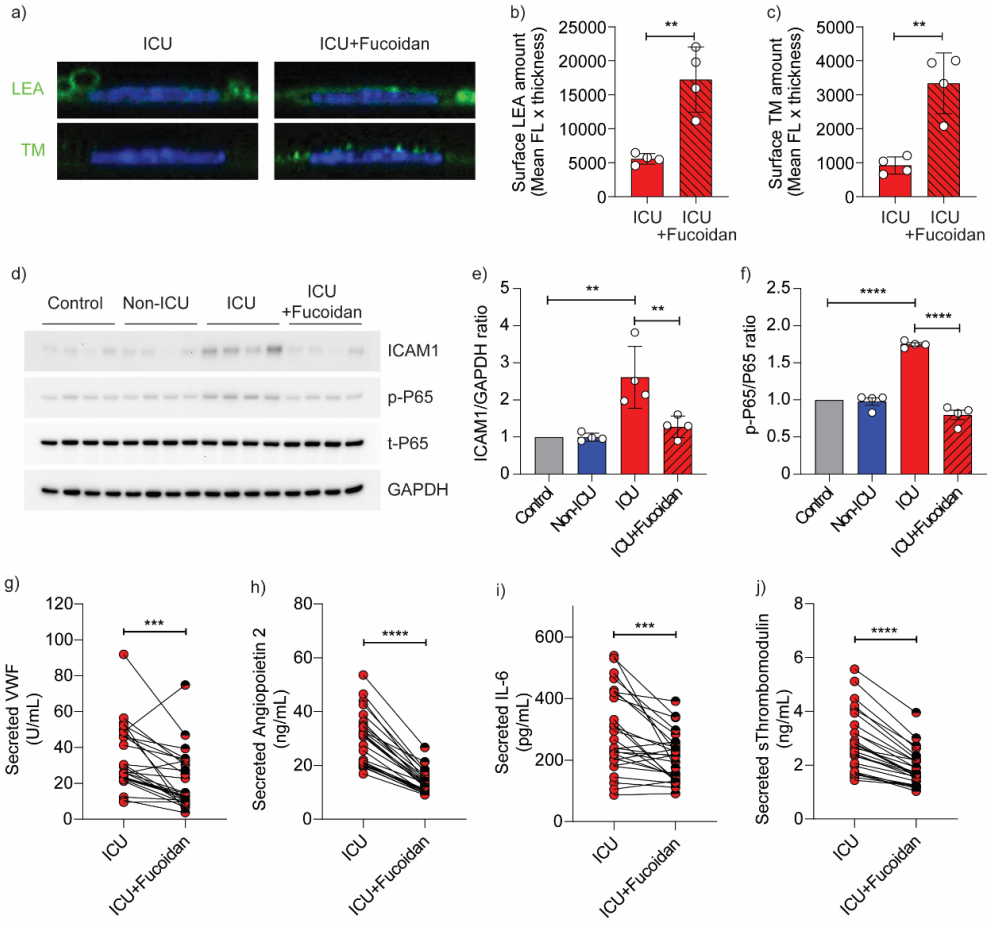

Figure 4 Fucoidan restores glycocalyx thickness on HPMECs and reduces endothelial activation. a) Representative confocal images of *Lycopersicon esculentum*-FITC (LEA) or anti-thrombomodulin (TM) staining on the surface of primary human pulmonary microvascular endothelial cells (HPMECs) in the presence of 10% pooled COVID-19 ICU (n

= 26) serum with and without fucoidan (10 µg/mL) for 24hrs. Quantification of HPMECs surface b) LEA and c) TM expression in the presence of 10% pooled COVID-19 ICU serum with and without fucoidan (10 µg/mL) for 24hrs of 4 independent experiments. d) Western blot images of ICAM1, p-P65, t-P65 protein expression. Quantification of e) ICAM1/GAPDH ratio and f) p-P65/t-P65 ratio in HPMECs in response to 10% pooled-healthy control (n = 12), COVID-19 non-ICU (n = 8) and COVID-19 ICU (n = 26) serum with and without fucoidan (10 µg/mL) for 24hrs of 4 independent experiments, presented as fold change expression normalized to healthy control. Secreted g) VWF, h) angiopoietin 2, i) IL6 and j) soluble thrombomodulin of HPMECs stimulated with 10% individual COVID-19 ICU sera (n = 26) with and without fucoidan (10 µg/mL) for 24hrs. One-way ANOVA followed by Tukey's multiple comparisons test, Kruskal-Wallis test followed by Dunn's multiple comparisons test and paired two-tailed Student t test were performed; *p<0.05, **p<0.01, ***p<0.001, ****p<0.0001.

Glycocalyx restoration could protect endothelial cell barrier function

As fucoidan supplementation could restore the glycocalyx and reduce inflammation we used ECIS to further investigate the effects of fucoidan on protection of the endothelial barrier function. After 24hrs of culturing the HPMECs with the various serum samples, addition of fucoidan had no effect during the first 7-8hrs. However, in the following time period, endothelial barrier integrity of HPMECs exposed to serum from COVID-19 ICU patients recovered significantly (figure 5a-d). Several samples even reached similar levels as control samples (figure 5b,d). Additionally, VE-cadherin and F-actin staining also showed a similar trend that fucoidan could strengthen the cell-cell contacts against COVID-19 ICU serum exposure (figure 5e,f).

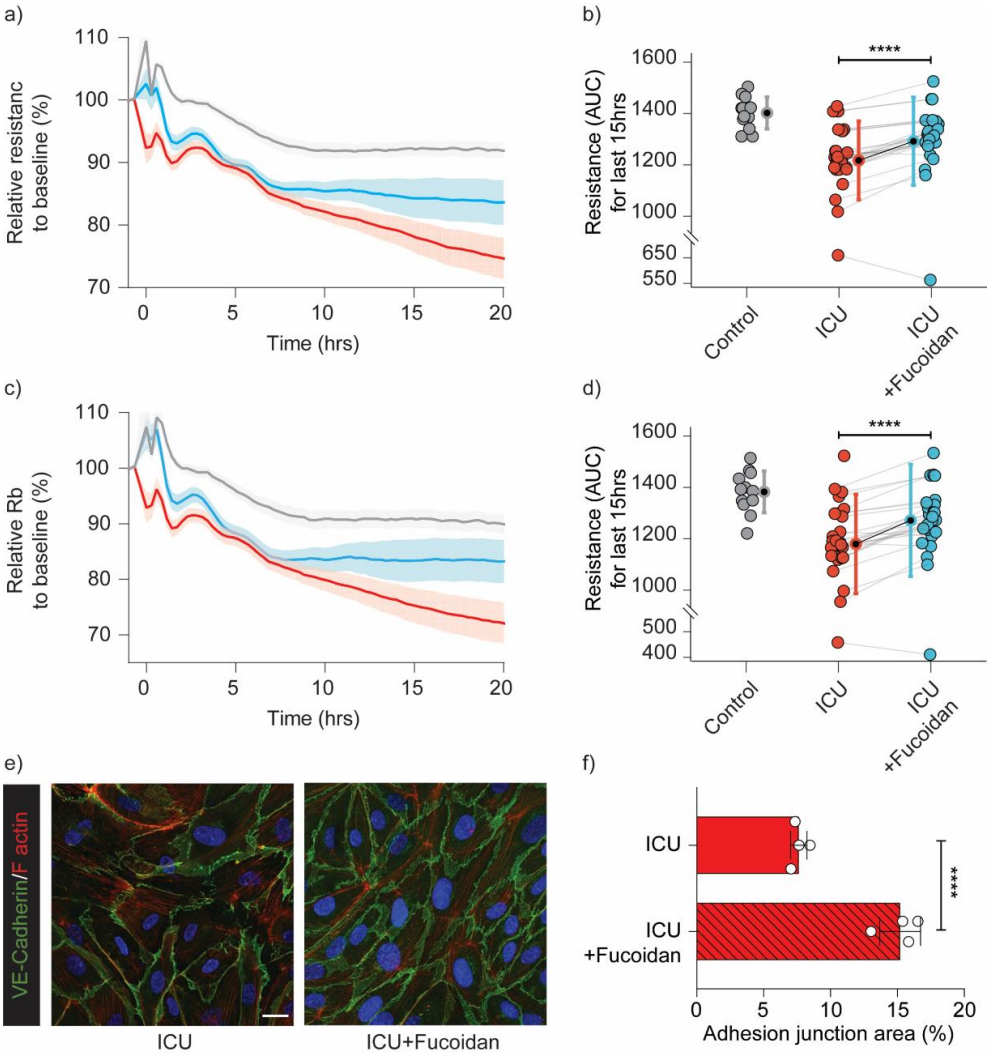

Figure 5 Fucoidan could ameliorate endothelial cell barrier function in presence of serum of COVID-19 ICU patients. a) Barrier integrity parameter, resistance of a) primary human pulmonary microvascular endothelial cells (HPMECs) assessed by ECIS in response to stimulation with 10% serum (at t=0hr) of healthy controls (n=12, grey line), COVID-19 ICU (n=26, red line) and COVID-19 ICU with fucoidan (n=26, blue line). Cell-cell contact parameter, Rb of c) primary human pulmonary microvascular endothelial cells (HPMECs) assessed by ECIS in response to stimulation with 10% serum (at t=0hr) of healthy controls (n=12, grey line), COVID-19 ICU (n=26, red line) and COVID-19 ICU with fucoidan (n=26, blue line). Data were normalized to the baseline resistance or Rb to calculate the relative resistance or Rb to baseline (%) and presented as mean ± SEM. b) Quantification of barrier

integrity was based on the measurements of area under curve of final 15 hours. d) Quantification of cell-cell contact was based on the measurements of area under curve of final 15 hours. e) Representative confocal images of VE-cadherin (green) and F-actin (red) staining on HPMECs in the presence of 10% pooled COVID-19 ICU serum with and without fucoidan (10 μg/mL) for 24hr (scale bar = 20 μm). f) Quantification of adhesion junction percentage of HPMECs in the presence of 10% pooled COVID-19 ICU serum with and without fucoidan (10 μg/mL) for 24hr of 4 independent experiments. Graphs represent the mean ± SD. Nonpaired and paired two-tailed Student t test were performed; ****p<0.0001.

Fucoidan inhibits the formation of a procoagulant cell surface upon COVID-19 serum treatment

To test whether serum from COVID-19 ICU patient is capable of inducing a procoagulant cell surface, explaining the reported high incidence of (micro)thrombosis in COVID-19 ICU patients [20], we first examined tissue factor (TF) gene expression (*F3*) changes. Indeed, *F3* was significantly upregulated in COVID-19 ICU patient samples (supplementary figure S5a) and the presence of fucoidan normalized this expression again to control levels. Next, the production of factor Xa on endothelial cell surface was induced by 10% serum from healthy controls and COVID-19 patients (figure 6a) which resulted in a significant increase in factor Xa production in COVID-19 ICU samples compared to samples from healthy controls and COVID-19 non-ICU, indicating the formation of procoagulant cell surface (supplementary figure S5b,c). Consistent with the observed reduction in *F3* mRNA expression with fucoidan present, FX activation was considerably reduced within 1 hour and 2 hours (figure 6b,c).

Thrombin release (figure 6d), another product of the common coagulation pathway, was significantly increased in the COVID-19 ICU group, indicating serum from ICU patients could lead to EC hypercoagulable state (supplementary figure S5d). When comparing the COVID-19 ICU groups with and without fucoidan added, thrombin peak height, similar to the phenotype in Xa generation assay, showed a significant decrease in fucoidan treated COVID-19 ICU samples (figure 6f). Correlating FXa and thrombin generation with the

plasma levels of ANG2, sTM and sSDC1, we found there's a link between endothelial activation, glycocalyx degradation and EC surface coagulable state (figure 6g).

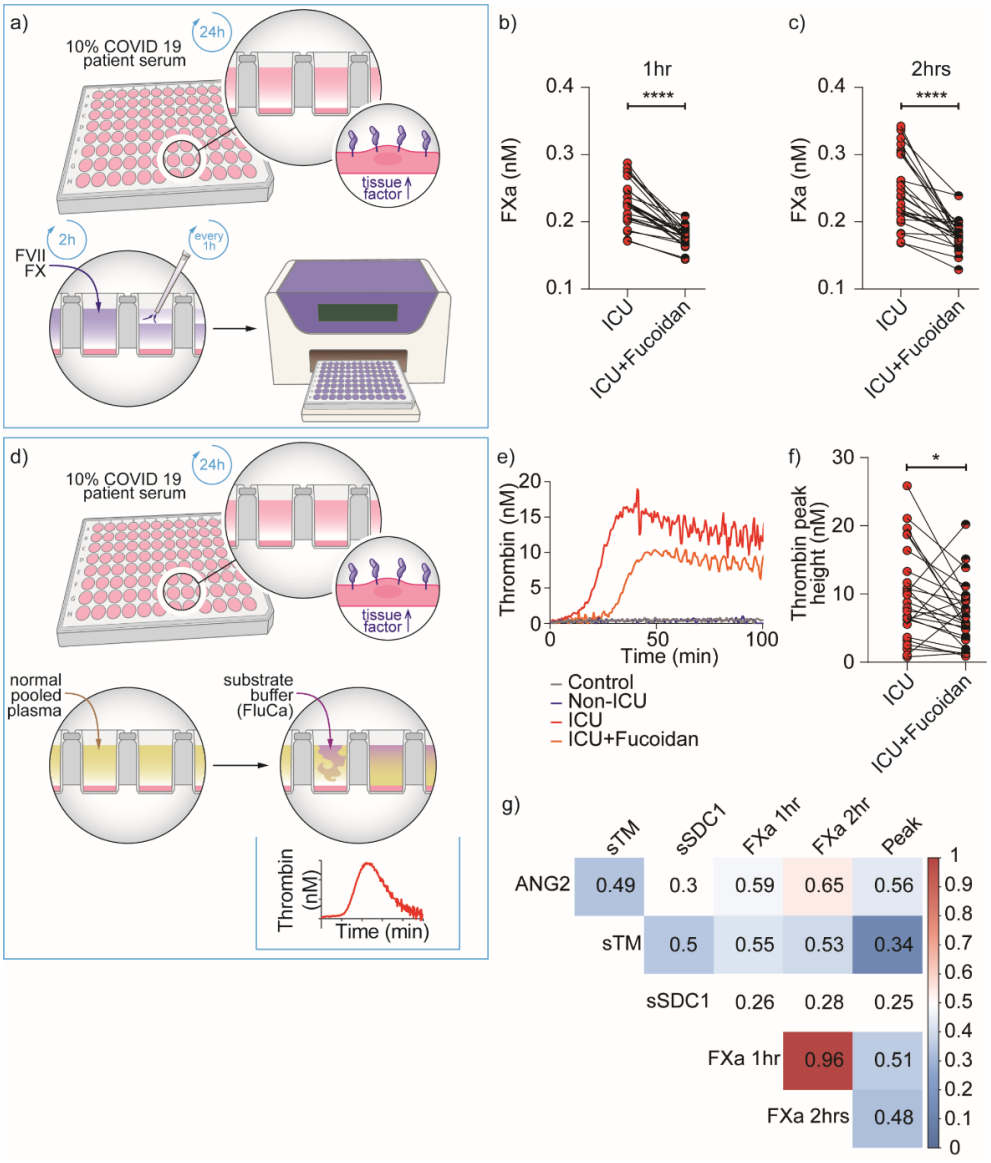

Figure 6 Fucoidan inhibits the formation of procoagulant cell surface in response to serum of COVID-19 ICU patients. a) Schematic overview showing how to detect FX activation on HPMEC cell surface in response to 10% healthy control or COVID-19 serum.

FXa production (nM) in b) first hour and c) second hour on HPMECs surface in the presence of 10% individual COVID-19 ICU sera (n = 26) with and without fucoidan (10 µg/mL) for 24hrs. d) Schematic overview showing how to detect thrombin generation on HPMECs cell surface in response to 10% healthy control or COVID-19 serum. e) Representative graph of thrombin generation assay in the presence of 10% healthy control, COVID-19 non-ICU, and COVID-19 ICU with and without fucoidan (same serum induced cell surface). f) Thrombin generation peak height (nM) measured on HPMECs surface in the presence of 10% individual COVID-19 ICU serum (n = 26) with and without fucoidan (10 µg/mL) for 24hrs. g) Pearson's correlation heatmap between endothelial dysfunction and glycocalyx shedding related markers (angiopoietin-2, soluble thrombomodulin and soluble syndecan-1) and coagulation assay parameters (FXa 1hr, FXa 2hr and thrombin peak height). Colours represent correlation, blue means negative correlated and red means positive correlated. Blank means no significance. Graphs represent the mean ± SD and paired two-tailed Student t test were performed; *p<0.05, ****p<0.0001.

Discussion

Our current study underpins the critical role for loss of the endothelial glycocalyx in severe COVID-19 infections. At a patient level, the endothelial activation marker ANG2 and glycocalyx shedding related markers sTM and sSDC1 were all increased in COVID-19 patients in ICU. At a cellular level, the loss of the endothelial glycocalyx induced by sera of these patients resulted in cellular activation, increased permeability and a hypercoagulable surface. Intervention with the HS-mimetic fucoidan restored not only the endothelial glycocalyx but subsequently reduced the endothelial activation state and restored the permeability barrier and anti-coagulant cell surface.

Increased circulating ANG2 levels have been associated with diminished respiratory function, increased coagulation activity, acute kidney injury and higher mortality in COVID-19 patients [18, 21-23]. Inhibition of the protective ANG1/TIE2 signalling cascade by ANG2 is a central regulator in protecting the vasculature against thrombus formation and vascular stabilization [24, 25]. Consistent with our findings, a decrease in plasma ANG2 levels upon recovery argues for ANG2 as a sensitive marker for acute endothelial dysfunction. The observed lower ANG2 levels in our study, together with the relative low

levels of sTM and sSDC1, in comparison to non-COVID-19 septic ICU patients, could argue that COVID-19 is a more locally presenting disease [26]. sTM has been reported to be associated with COVID-19 adverse outcome [27] and loss of endothelial surface TM was observed in COVID-19 lung autopsies [28]. We observed that once the microvascular lung endothelial cells were activated, the relatively highly expressed TM (supplementary figure S6) was shed, resulting in a procoagulant cell surface that indicates possible local vulnerability of lung microvessels.

We previously revealed that increased breakdown of HS by heparanase could lead to diminished glycocalyx coverage [29]. Further studies suggest that heparanase activity, the only mammalian enzyme which could degrade HS, was elevated in COVID-19 patients and associated with disease severity [17, 30]. Our observation of increased *HPSE-1* mRNA expression upon ICU COVID-19 serum treated ECs corresponded with reduced LEA-FITC, HS and TM surface expression [31], the induced upregulation of ANG2 and heparanase and loss of EC barrier function. These findings provide increasing evidence linking endothelial glycocalyx as an additional component of vascular barrier with the ANG/TIE2 signalling pathway to maintain EC homeostasis. Additionally, lung microvascular endothelial cells were more sensitive to COVID-19 ICU serum than glomerular microvascular endothelial cells, emphasizing that organs are differently affected by COVID-19 infection. Notably, the indirect effect by serum mediators, as was also suggested in recent papers [32, 33] in addition to possible direct viral infection, might contribute to patients' longer hospitalization or driving the disease progression to severe ARDS.

Coagulation disorder is often seen in COVID-19, especially in severe cases [34]. The endothelial glycocalyx is a crucial compartment for binding and regulating enzymes involved in the coagulation cascade [35]. Tissue factor is a primary trigger of extrinsic coagulation and plays an essential role in haemostasis, which is increased as a result of glycocalyx damage [36, 37]. Combining with our data, the increased endothelial *F3* expression corresponded with loss of the endothelial anticoagulant factors, such as TM, in

response to incubation with COVID-19 ICU patient serum. This may be a driver of COVID-19 related coagulopathy, which is corroborated by two different *ex vivo* assays (thrombin generation and Xa generation on endothelial cell surface).

Here we observed that restoration of glycocalyx components by fucoidan leads to reduction of endothelial activation through inactivation of NFκB signalling pathway and downstream ICAM1 expression. Additionally, supplementary fucoidan induced endothelial barrier function recovery which might open a new therapeutic strategy to treat or prevent respiratory dysfunction. Moreover, fucoidan supplementation has beneficial effect for anticoagulation. First of all, fucoidan leads to EC surface TF reduction. Two preprint studies suggested that ANG2 has additional and direct effects on coagulation in COVID-19 [28, 38], and our data demonstrates that fucoidan has a strong effect on decreasing ANG2 expression, preventing TIE2 inactivation. These findings reveal that glycocalyx preservation has promising effects on controlling COVID-19 injury and our in vitro experiments show fucoidan as a novel HS mimetic could be a potential therapeutic substance.

Our study had some limitations due to the time of hospitalization of COVID-19 patients and official ethical approval. The present study only presents a limited group of patients who presented at the LUMC during the first wave before major changes in therapeutic interventions occurred, such as the inclusion of dexamethasone treatment. In addition, no non-COVID-19 ARDS ICU patients were included, limiting the attribution of our data as COVID-19 specific effects. However, similar lung mechanics and increased extravascular lung edema in COVID-19 related ARDS in comparison to non-COVID-19 ARDS have been found, indicating a similar contribution found in our study [39]. In addition, the Fucoidan we used in the present study, by itself was not intended to be for clinical use, but to exemplify possible glycocalyx restoring mechanisms and endothelial cell functionality.

In conclusion, our present study supports the concept that endothelial cell dysfunction and loss of endothelial glycocalyx might drive worse outcomes like ARDS or coagulopathy

in severe COVID-19 at later disease stage. Fucoidan restored the endothelial glycocalyx, ameliorated endothelial activation, which led to protection of endothelial barrier function and induced antithrombotic effects. Our findings support further validation whether glycocalyx preservation or restoration could prevent progression to severe COVID-19 and encourage more clinical trials to evaluate the efficacy of glycocalyx preservation for treatment of more severe forms of COVID-19.

Acknowledgements

We thank all patients and healthy volunteers for taking part in this study. The fucoidan, a main ingredient of the Endocalyx™ supplement (US patent # 9943572), is exclusively produced for MicroVascular Health Solutions LLC and was provided as a gift.

Author contributions

L. Yuan, T.J. Rabelink and B.M. van den Berg conceived and designed the study; L. Yuan, S. Chen, W.M.P.J. Sol and B.M. van den Berg performed experiments and original data collection; L. Yuan, T.J. Rabelink and B.M. van den Berg analysed and interpreted the data; L. Yuan, A.I.M. van der Velden, H. Vink, T.J. Rabelink and B.M. van den Berg edited and discussed the manuscript.

Support statement

This work was supported by the China Scholarship Council grant to L. Yuan (CSC number 201806270262) and BEAT-COVID funding by Leiden University Medical Center.

Availability of data and materials

All data and methods supporting the findings of this study are available from the corresponding author upon reasonable request.

Competing interests

The authors declare that they have no relevant financial interests or personal relationships.

Conflict of interest

L. Yuan reports support for the present manuscript received from the China Scholarship Council grant CSC number 201806270262. H. Vink is Chief Science Officer of MicroVascular Health Solutions LLC (Alpine, UT, USA) and reports the Endocalyx patent (number 9943572) granted to MicroVascular Health Solutions in 2018. The remaining authors have nothing to disclose.

Consent for publication

The manuscript was approved by all authors for publication.

Reference

1. Cascella M, Rajnik M, Aleem A, Dulebohn SC, Di Napoli R. Features, Evaluation, and Treatment of Coronavirus (COVID-19). StatPearls, Treasure Island (FL), 2021.

2. Huang C, Wang Y, Li X, Ren L, Zhao J, Hu Y, Zhang L, Fan G, Xu J, Gu X, Cheng Z, Yu T, Xia J, Wei Y, Wu W, Xie X, Yin W, Li H, Liu M, Xiao Y, Gao H, Guo L, Xie J, Wang G, Jiang R, Gao Z, Jin Q, Wang J, Cao B. Clinical features of patients infected with 2019 novel coronavirus in Wuhan, China. *Lancet* 2020: 395(10223): 497-506.

3. Ferrando C, Suarez-Sipmann F, Mellado-Artigas R, Hernandez M, Gea A, Arruti E, Aldecoa C, Martinez-Palli G, Martinez-Gonzalez MA, Slutsky AS, Villar J, Network C-SI. Clinical features, ventilatory management, and outcome of ARDS caused by COVID-19 are

similar to other causes of ARDS. *Intensive Care Med* 2020: 46(12): 2200-2211.

4. Grasselli G, Zangrillo A, Zanella A, Antonelli M, Cabrini L, Castelli A, Cereda D, Coluccello A, Foti G, Fumagalli R, Iotti G, Latronico N, Lorini L, Merler S, Natalini G, Piatti A, Ranieri MV, Scandroglio AM, Storti E, Cecconi M, Pesenti A, Network C-LI. Baseline Characteristics and Outcomes of 1591 Patients Infected With SARS-CoV-2 Admitted to ICUs of the Lombardy Region, Italy. *JAMA* 2020: 323(16): 1574-1581.

5. Cui S, Chen S, Li X, Liu S, Wang F. Prevalence of venous thromboembolism in patients with severe novel coronavirus pneumonia. *J Thromb Haemost* 2020: 18(6): 1421-1424.

6. Zhou F, Yu T, Du R, Fan G, Liu Y, Liu Z, Xiang J, Wang Y, Song B, Gu X, Guan L, Wei Y, Li H, Wu X, Xu J, Tu S, Zhang Y, Chen H, Cao B. Clinical course and risk factors for mortality of adult inpatients with COVID-19 in Wuhan, China: a retrospective cohort study. *Lancet* 2020: 395(10229): 1054-1062.

7. Vassiliou AG, Kotanidou A, Dimopoulou I, Orfanos SE. Endothelial Damage in Acute Respiratory Distress Syndrome. *Int J Mol Sci* 2020: 21(22).

8. Vallet B, Wiel E. Endothelial cell dysfunction and coagulation. *Crit Care Med* 2001: 29(7 Suppl): S36-41.

9. Ackermann M, Verleden SE, Kuehnel M, Haverich A, Welte T, Laenger F, Vanstapel A, Werlein C, Stark H, Tzankov A, Li WW, Li VW, Mentzer SJ, Jonigk D. Pulmonary Vascular Endothelialitis, Thrombosis, and Angiogenesis in Covid-19. *N Engl J Med* 2020: 383(2): 120-128.

10. van den Berg BM, Wang G, Boels MGS, Avramut MC, Jansen E, Sol W, Lebrin F, van Zonneveld AJ, de Koning EJP, Vink H, Grone HJ, Carmeliet P, van der Vlag J, Rabelink TJ. Glomerular Function and Structural Integrity Depend on Hyaluronan Synthesis by Glomerular Endothelium. *J Am Soc Nephrol* 2019: 30(10): 1886-1897.

11. Rabelink TJ, van den Berg BM, Garsen M, Wang G, Elkin M, van der Vlag J. Heparanase: roles in cell survival, extracellular matrix remodelling and the development of kidney disease. *Nature reviews Nephrology* 2017: 13(4): 201-212.

12. Wang G, Kostidis S, Tiemeier GL, Sol W, de Vries MR, Giera M, Carmeliet P, van den Berg BM, Rabelink TJ. Shear Stress Regulation of Endothelial Glycocalyx Structure Is Determined by Glucobiosynthesis. *Arteriosclerosis, thrombosis, and vascular biology* 2020: 40(2): 350-364.

13. Wang G, de Vries MR, Sol W, van Oeveren-Rietdijk AM, de Boer HC, van Zonneveld AJ, Quax PHA, Rabelink TJ, van den Berg BM. Loss of Endothelial Glycocalyx Hyaluronan Impairs Endothelial Stability and Adaptive Vascular Remodeling After Arterial Ischemia. *Cells* 2020: 9(4).

14. Boels MG, Lee DH, van den Berg BM, Dane MJ, van der Vlag J, Rabelink TJ. The endothelial glycocalyx as a potential modifier of the hemolytic uremic syndrome.

European journal of internal medicine 2013: 24(6): 503-509.

15. Uchimido R, Schmidt EP, Shapiro NI. The glycocalyx: a novel diagnostic and therapeutic target in sepsis. *Critical care* 2019: 23(1): 16.

16. Rovas A, Sackarnd J, Rossaint J, Kampmeier S, Pavenstadt H, Vink H, Kumpers P. Identification of novel sublingual parameters to analyze and diagnose microvascular dysfunction in sepsis: the NOSTRADAMUS study. *Critical care* 2021: 25(1): 112.

17. Buijsers B, Yanginlar C, de Nooijer A, Grondman I, Maciej-Hulme ML, Jonkman I, Janssen NAF, Rother N, de Graaf M, Pickkers P, Kox M, Joosten LAB, Nijenhuis T, Netea MG, Hilbrands L, van de Veerdonk FL, Duivenvoorden R, de Mast Q, van der Vlag J. Increased Plasma Heparanase Activity in COVID-19 Patients. *Frontiers in immunology* 2020: 11: 575047.

18. Rovas A, Osiaevi I, Buscher K, Sackarnd J, Tepasse PR, Fobker M, Kuhn J, Braune S, Gobel U, Tholking G, Groschel A, Pavenstadt H, Vink H, Kumpers P. Microvascular dysfunction in COVID-19: the MYSTIC study. *Angiogenesis* 2021: 24(1): 145-157.

19. Wang J, Zhang Q, Zhang Z, Zhang H, Niu X. Structural studies on a novel fucogalactan sulfate extracted from the brown seaweed Laminaria japonica. *International journal of biological macromolecules* 2010: 47(2): 126-131.

20. McFadyen JD, Stevens H, Peter K. The Emerging Threat of (Micro)Thrombosis in COVID-19 and Its Therapeutic Implications. *Circ Res* 2020: 127(4): 571-587.

21. Vassiliou AG, Keskinidou C, Jahaj E, Gallos P, Dimopoulou I, Kotanidou A, Orfanos SE. ICU Admission Levels of Endothelial Biomarkers as Predictors of Mortality in Critically Ill COVID-19 Patients. *Cells* 2021: 10(1).

22. Henry BM, de Oliveira MHS, Cheruiyot I, Benoit JL, Cooper DS, Lippi G, Le Cras TD, Benoit SW. Circulating level of Angiopoietin-2 is associated with acute kidney injury in coronavirus disease 2019 (COVID-19). *Angiogenesis* 2021.

23. Smadja DM, Guerin CL, Chocron R, Yatim N, Boussier J, Gendron N, Khider L, Hadjadj J, Goudot G, Debuc B, Juvin P, Hauw-Berlemont C, Augy JL, Peron N, Messas E, Planquette B, Sanchez O, Charbit B, Gaussem P, Duffy D, Terrier B, Mirault T, Diehl JL. Angiopoietin-2 as a marker of endothelial activation is a good predictor factor for intensive care unit admission of COVID-19 patients. *Angiogenesis* 2020: 23(4): 611-620.

24. Lovric S, Lukasz A, Hafer C, Kielstein JT, Haubitz M, Haller H, Kumpers P. Removal of elevated circulating angiopoietin-2 by plasma exchange--a pilot study in critically ill patients with thrombotic microangiopathy and anti-glomerular basement membrane disease. *Thromb Haemost* 2010: 104(5): 1038-1043.

25. Higgins SJ, De Ceunynck K, Kellum JA, Chen X, Gu X, Chaudhry SA, Schulman S, Libermann TA, Lu S, Shapiro NI, Christiani DC, Flaumenhaft R, Parikh SM. Tie2 protects the vasculature against thrombus formation in systemic inflammation. *J Clin Invest* 2018:

128(4): 1471-1484.

26. Bhatraju PK, Morrell ED, Zelnick L, Sathe NA, Chai XY, Sakr SS, Sahi SK, Sader A, Lum DM, Liu T, Koetje N, Garay A, Barnes E, Lawson J, Cromer G, Bray MK, Pipavath S, Kestenbaum BR, Liles WC, Fink SL, West TE, Evans L, Mikacenic C, Wurfel MM. Comparison of host endothelial, epithelial and inflammatory response in ICU patients with and without COVID-19: a prospective observational cohort study. *Crit Care* 2021: 25(1): 148.

27. Goshua G, Pine AB, Meizlish ML, Chang CH, Zhang H, Bahel P, Baluha A, Bar N, Bona RD, Burns AJ, Dela Cruz CS, Dumont A, Halene S, Hwa J, Koff J, Menninger H, Neparidze N, Price C, Siner JM, Tormey C, Rinder HM, Chun HJ, Lee AI. Endotheliopathy in COVID-19-associated coagulopathy: evidence from a single-centre, cross-sectional study. *Lancet Haematol* 2020: 7(8): e575-e582.

28. Schmaier AA, Hurtado GP, Manickas-Hill ZJ, Sack KD, Chen SM, Bhambhani V, Quadir J, Nath AK, Collier AY, Ngo D, Barouch DH, Gerszten RE, Yu XG, Collection MC-, Processing T, Peters K, Flaumenhaft R, Parikh SM. Tie2 activation protects against prothrombotic endothelial dysfunction in COVID-19. *medRxiv* 2021.

29. Boels MG, Avramut MC, Koudijs A, Dane MJ, Lee DH, van der Vlag J, Koster AJ, van Zonneveld AJ, van Faassen E, Grone HJ, van den Berg BM, Rabelink TJ. Atrasentan Reduces Albuminuria by Restoring the Glomerular Endothelial Glycocalyx Barrier in Diabetic Nephropathy. *Diabetes* 2016: 65(8): 2429-2439.

30. Potje SR, Costa TJ, Fraga-Silva TFC, Martins RB, Benatti MN, Almado CEL, de Sa KSG, Bonato VLD, Arruda E, Louzada-Junior P, Oliveira RDR, Zamboni DS, Becari C, Auxiliadora-Martins M, Tostes RC. Heparin prevents in vitro glycocalyx shedding induced by plasma from COVID-19 patients. *Life sciences* 2021: 276: 119376.

31. Stahl K, Gronski PA, Kiyan Y, Seeliger B, Bertram A, Pape T, Welte T, Hoeper MM, Haller H, David S. Injury to the Endothelial Glycocalyx in Critically Ill Patients with COVID-19. *Am J Respir Crit Care Med* 2020: 202(8): 1178-1181.

32. Birnhuber A, Fliesser E, Gorkiewicz G, Zacharias M, Seeliger B, David S, Welte T, Schmidt J, Olschewski H, Wygrecka M, Kwapiszewska G. Between inflammation and thrombosis - endothelial cells in COVID-19. *The European respiratory journal : official journal of the European Society for Clinical Respiratory Physiology* 2021.

33. Michalick L, Weidenfeld S, Grimmer B, Fatykhova D, Solymosi PD, Behrens F, Dohmen M, Brack MC, Schulz S, Thomasch E, Simmons S, Muller-Redetzky H, Suttorp N, Kurth F, Neudecker J, Toennies M, Bauer TT, Eggeling S, Corman VM, Hocke AC, Witzenrath M, Hippenstiel S, Kuebler WM. Plasma mediators in patients with severe COVID-19 cause lung endothelial barrier failure. *The European respiratory journal : official journal of the European Society for Clinical Respiratory Physiology* 2021: 57(3).

34. Iba T, Levy JH, Levi M, Thachil J. Coagulopathy in COVID-19. *J Thromb Haemost* 2020: 18(9): 2103-2109.

35. Nieuwdorp M, van Haeften TW, Gouverneur MC, Mooij HL, van Lieshout MH, Levi M, Meijers JC, Holleman F, Hoekstra JB, Vink H, Kastelein JJ, Stroes ES. Loss of endothelial glycocalyx during acute hyperglycemia coincides with endothelial dysfunction and coagulation activation in vivo. *Diabetes* 2006: 55(2): 480-486.

36. Grover SP, Mackman N. Tissue Factor: An Essential Mediator of Hemostasis and Trigger of Thrombosis. *Arterioscler Thromb Vasc Biol* 2018: 38(4): 709-725.

37. Ramnath R, Foster RR, Qiu Y, Cope G, Butler MJ, Salmon AH, Mathieson PW, Coward RJ, Welsh GI, Satchell SC. Matrix metalloproteinase 9-mediated shedding of syndecan 4 in response to tumor necrosis factor alpha: a contributor to endothelial cell glycocalyx dysfunction. *FASEB J* 2014: 28(11): 4686-4699.

38. Hultström M, Fromell K, Larsson A, Quaggin SE, Betsholtz C, Frithiof R, Lipcsey M, Jeansson M. Elevated Angiopoietin-2 inhibits thrombomodulin-mediated anticoagulation in critically ill COVID-19 patients. *medRxiv* 2021: 2021.2001.2013.21249429.

39. Shi R, Lai C, Teboul JL, Dres M, Moretto F, De Vita N, Pham T, Bonny V, Mayaux J, Vaschetto R, Beurton A, Monnet X. COVID-19 ARDS is characterized by higher extravascular lung water than non-COVID-19 ARDS: the PiCCOVID study. *Critical Care* 2021: 25(1).

Supporting information

Supplementary Material and methods

Circulating markers of endothelial dysfunction and glycocalyx shedding

Plasma samples were thawed at room temperature. All plasma analytes were measured with immunoassays in duplicate according to manufacturer's recommendation. Samples were diluted in diluent reagent according to manufacturer's protocol. Analytes measured include angiopoietin 2 (Ang-2, DANG20, R&D Systems, Abingdon, UK), soluble thrombomodulin (sTM, M850720096, Diaclone, Besançon, France) and soluble syndecan-1 (sSDC1, DY2780, R&D Systems). For angiopoietin 2 and soluble thrombomodulin, commercial control samples were included in each plate to confirm the amount of protein level.

***In Vitro* Culture Experiments**

Primary human pulmonary microvascular endothelial cells (HPMECs) were purchased from PromoCell (Lot no. 455Z003, Heidelberg, Germany) and primary human glomerular microvascular ECs (GEnCs) were purchased from Cell Systems (ACBRI-128; Kirkland, WA, USA) and were both cultured in endothelial growth medium (basal medium MV, C-22220, PromoCell) supplemented with C-39220 (PromoCell) and 1% antibiotics (penicillin/streptomycin, 15070063, Gibco, Paisley, UK) at 37°C and 5% CO_2. For each cell line, passage 5 were used for experiments.

Endothelial barrier function assay

Endothelial barrier function analysis was performed with impedance-based cell monitoring using the electric cell-substrate impedance sensing system (ECIS Zθ, Applied

Biophysics, New York, USA). ECIS plates (96W20idf PET, Applied Biophysics) were pre-treated with 10 mM L-cysteine and coated with 1% gelatine (for GEnCs) or without 1% gelatine (for HPMECs). HPMECs (p5) were seeded at a concentration of 4.5×10^5 cells/well and for GEnCs (p5), the concentration was 3×10^5 cells/well. Medium was refreshed after 24 hours. Initial baseline resistance was measured for 2 hours before endothelial cells were seeded into the plate. Multiple frequency/time mode was used for the real-time assessment of the barrier function. Additionally, the real-time resistance was generated every 350 seconds. Once the stable monolayer was formed, endothelial cells were incubated with 10% serum (healthy (n=12), COVID-19 non-ICU (n=8) and ICU (n=26)) and measured for 20 hours. Afterwards, modelling data Rb which represents barrier function could be generated.

In additional experiments, HPMECs were exposed to 10% healthy serum (n=12), COVID-19 ICU serum (n=26) with or without fucoidan (10 µg/mL, gift from MicroVascular Health Solutions LLC, Alpine, UT, USA) and measured on the ECIS machine for 20 hours. The natural fucoidan provided (Iso 9000 and GMP certified from Omnipharm, S.A.S, Chambéry, France) was extracted from *Laminaria japonica* as a powder of 91.20% purity and further tested, for instance, on the presence of heavy metals (arsenic, lead, cadmium, mercury) or microbiology parameters (European Pharmacopoeia VIII, Ed 2,6,12: total plate count, yeast, mold, *E. coli, Salmonella spp.*). A 50x times stock solution was prepared by dissolving the appropriate amount of powder in milliQ water and passed through a 0.22µm filter before use. Cell culturing supernatant and 10% serum in no FCS medium were collected and centrifuged for VWF ELISA assay.

RNA isolation and RT-PCR

Cells were harvested in TRIzol and total RNA was isolated using RNeasy Mini Kit (74106, Qiagen, Venlo, The Netherlands) according to its protocol. cDNA synthesis was transcribed

using GoScript™ Reverse Transcriptase kit (A5001, Promega, Leiden, The Netherlands). RT-PCR analysis was conducted using SYBR Select Master Mix (4472908, Applied Biosystems, Landsmeer, The Netherlands) and specific primers as indicated in supplementary table s2. Gene expression was normalized to GAPDH of 5 separate experiments.

Immunoblotting analysis

Western blots were performed from protein extracts of HPMECs. Cells were washed once with cold PBS and lysed in lysis buffer mentioned in our previous study[1]. After centrifugation of the samples at 12,000 rpm for 15 min at 4°C, supernatant was collected and protein concentration was measured using the Pierce BCA Protein Assay Kit (23255, ThermoFisher, Landsmeer, The Netherlands). Equal amounts of protein were denatured using DTT and incubated at 95°C for 10 minutes. 10% Mini-PROTEAN® TGX™ Protein Gels (4561031, Bio-Rad Laboratories, Veenendaal, The Netherlands) were used for protein size separation and proteins were transferred to PVDF membranes (1704156, Bio-Rad) using the Trans-Blot Turbo system. Afterwards, the membrane was blocked in 5% milk in PBST at room temperature for 1 hour. Primary antibody rabbit anti-human ICAM1 (4915, Cell Signalling Technology), rabbit anti-human total NF-κB p65 (8242, Cell Signalling Technology), rabbit anti-human phosphor-NF-κB p65 (Ser536) (3033, Cell Signalling Technology) and mouse anti-human GAPDH (MA5-15738, ThermoFisher) were incubated overnight at 4°C. Incubation with a secondary HRP-conjugated antibody (P0447 and P0448, Dako, Amstelveen, The Netherlands) and visualization using Western Lightning Plus-ECL, Enhanced Chemiluminescence Substrate (NEL103001EA, PerkinElmer, Groningen, The Netherlands). Intensity of the bands were analysed using ImageJ software. Relative intensity was determined by levels of GAPDH.

Immunofluorescence of cultured cells

HPMECs (p5) were cultured in 8-well chamber slides (ibiTreat, µ-Slide 8 Well). Medium was refreshed after 24 hours to remove non-attached cells. When HPMECs formed a confluent monolayer after 48 hours, they were incubated with 10% pooled serum (healthy control (pooled n = 12), non-ICU (pooled n = 8) and ICU (pooled n = 26) in no FCS medium for 24 hours. Next, cells were fixed with 4% PFA and 0.2% Triton-X100 in HBSS or 4% PFA in HBSS (for HS and LEA staining) for 10 minutes at room temperature, washed twice with 1% BSA in HBSS, and blocked with 3% goat serum in HBSS for 1 hour at room temperature. Then, cells were incubated with FITC labelled *Lycopersicon esculentum* (LEA-FITC, L0401, Sigma, Houten, The Netherlands), primary monoclonal Mouse Anti-Human VE cadherin (55-7H1; BD Biosciences), monoclonal Mouse Anti-heparan sulfate (10E4, 370255-1, AMSBIO, Abingdon, UK) and monoclonal Mouse Anti-TM (MA5-11454, ThermoFisher) at 4°C overnight, followed by an appropriate secondary antibody and phalloidin-TRITC (VE-cadherin samples) for 1 hour, all in blocking buffer. Cells were subsequently washed and incubated with Hoechst 33528 (1/1,000) for 10 minutes at room temperature.

Cells were imaged using a LEICA SP8 WLL confocal microscope (Leica, Rijswijk, the Netherlands) to create image stacks. Fluorescent images were analysed using Image J software. To quantify the total area of VE-cadherin staining, all VE-cadherin derived fluorescent signal below a threshold was included in a mask. The value for the threshold intensity was kept the same for each field and then the positive area of VE-cadherin is quantified as adhesion junction area. 10 fields per experiment were imaged for every condition for further analysis to quantify the glycocalyx coverage, endothelial nuclear region was selected and the thickness of the glycocalyx was quantified by calculating the distance from the half-maximum signal of the nuclear staining at the luminal side to the half-maximum signal at the luminal end of the staining in the z-direction. Fluorescence intensity was calculated based on the average fluorescence intensity from the half-maximum signal of the nuclear staining at the luminal side to the half-maximum signal at the luminal end of the staining in the z-direction. Surface amount of glycocalyx was presented as mean fluorescence intensity (Mean FL) times luminal thickness.

FX activation by extrinsic tenase complex (TF-FVIIa)

Primary human pulmonary microvascular endothelial cells at passage 5 were seeded into 96 wells plates at a concentration of $2.5x10^4$ cells/well. Medium was refreshed after 24 hours and after 48 hours, HPMECs were incubated with 10% control (n=12), COVID-19 non-ICU (n=8) and ICU serum (n=26, with or without presence of fucoidan) in no FCS medium for 24 hours. Cell culture supernatants were collected and centrifuged for ELISA assays. Afterwards, cells were washed once with prewarmed HBSS with Ca^{2+}. Factor VIIa (80 µL, 10 nM, HCVIIA-0031, Haematologic Technologies, Huissen, The Netherlands) was added and incubated for 15 minutes at 37°C and 5%CO_2. Then the reaction system was initiated by adding factor X (80 µL, 400 nM, HCX-0050, Haematologic Technologies). The plate was kept in incubator to keep the reaction continuous and 2 time points were selected (1 hour and 2 hours) to detect the production of active factor X. Aliquots were taken and quenched in HBS supplemented with 50mM EDTA to stop the reaction. The amidolytic activity of each sample was determined by SpecXa conversion (250 µM), measuring the absorbance at 405 nm and the initial rates of chromogenic substrate hydrolysis were converted to nanomolar of product by reference to a corresponding FXa standard curve.

Thrombin generation Assay

Primary human pulmonary microvascular endothelial cells at passage 5 were seeded into 96 wells plates at a concentration of $2.5x10^4$ cells/well. Medium was refreshed after 24 hours and after 48 hours, HPMECs were incubated with 10% healthy (n=12), COVID-19 non-ICU (n=8) and ICU serum (n=26, with or without presence of fucoidan) in no FCS medium for 24 hours. Warm HBSS without Ca^{2+} was used to wash the cells once. Thrombin generation curves were obtained by supplementing normal pooled plasma. Thrombin

formation was initiated by adding substrate buffer (FluCa-kit, 86197, Thrombinoscope BV, Leiden, The Netherlands) to the plasma. The final reaction volume was 120 µL, of which 80 µL was plasma, 20 µL was HBSS/calibrator and 20 µL was substrate. Thrombin formation was determined every 30 s for 120 min and corrected for the calibrator using Thrombinoscope software.

Markers of endothelial dysfunction and glycocalyx shedding in cell cultured supernatant

Supernatants collected from experiments mentioned above and stored at -80°C were measured with immunoassays in duplicate according to manufacturer's recommendation. Analytes measured include angiopoietin 2 (Ang-2, DANG20, R&D Systems), soluble thrombomodulin (TM, M850720096, Diaclone), IL-6 (M9316, Sanquin, Amsterdam, The Netherlands) and VWF (A0082, Dako). Samples were diluted 1:100, 1:5, 1:10 and 1:200 respectively in diluent reagent. For angiopoietin 2 and soluble thrombomodulin, commercial control samples were included in each plate to confirm the amount of protein level.

Public database mining

To further study the role of thrombomodulin in endothelial cells from different vascular beds, datasets from EC atlas (https://endotheliomics.shinyapps.io/ec_atlas/ [2]) and NCBI Gene expression Omnibus (https://www.ncbi.nlm.nih.gov/geo/) were downloaded. We then determined Thbd expression in mice ECs from 11 organs. For human ECs, 2 datasets (GSE43475 [3] and GSE21212 [4]) were downloaded and processed with RMA background correction, log2 transformation and normalization in R. For annotation, we chose the gene with the highest expression as the gene symbol and annotated it via different annotation packages. Then THBD expression was detected in different EC lines.

References

1. Wang G, Kostidis S, Tiemeier GL, Sol W, de Vries MR, Giera M, Carmeliet P, van den Berg BM, Rabelink TJ. Shear Stress Regulation of Endothelial Glycocalyx Structure Is Determined by Glucobiosynthesis. *Arteriosclerosis, thrombosis, and vascular biology* 2020: 40(2): 350-364.

2. Kalucka J, de Rooij L, Goveia J, Rohlenova K, Dumas SJ, Meta E, Conchinha NV, Taverna F, Teuwen LA, Veys K, Garcia-Caballero M, Khan S, Geldhof V, Sokol L, Chen R, Treps L, Borri M, de Zeeuw P, Dubois C, Karakach TK, Falkenberg KD, Parys M, Yin X, Vinckier S, Du Y, Fenton RA, Schoonjans L, Dewerchin M, Eelen G, Thienpont B, Lin L, Bolund L, Li X, Luo Y, Carmeliet P. Single-Cell Transcriptome Atlas of Murine Endothelial Cells. *Cell* 2020: 180(4): 764-779 e720.

3. Aranguren XL, Agirre X, Beerens M, Coppiello G, Uriz M, Vandersmissen I, Benkheil M, Panadero J, Aguado N, Pascual-Montano A, Segura V, Prosper F, Luttun A. Unraveling a novel transcription factor code determining the human arterial-specific endothelial cell signature. *Blood* 2013: 122(24): 3982-3992.

4. Bhasin M, Yuan L, Keskin DB, Otu HH, Libermann TA, Oettgen P. Bioinformatic identification and characterization of human endothelial cell-restricted genes. *BMC Genomics* 2010: 11: 342.

Graphic abstract

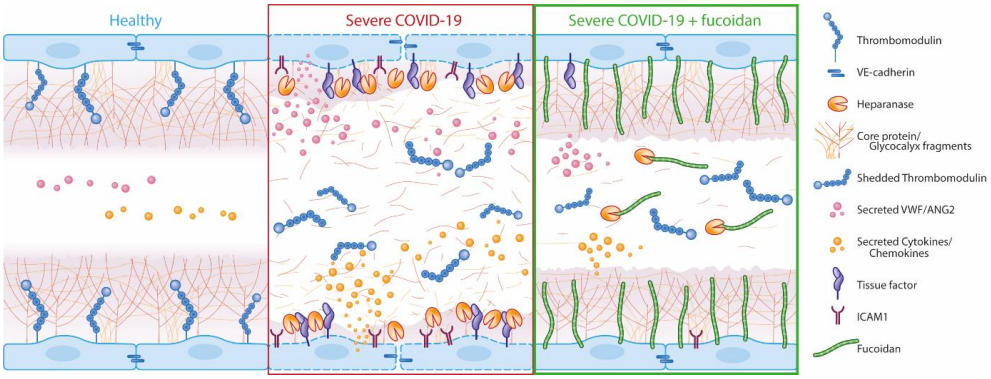

Under homeostatic conditions (healthy), intact endothelial glycocalyx maintains a stable endothelial barrier. COVID-19 serum of patients on ICU induces endothelial activation (cytokine release, ANG2 and VWF and shedding of thrombomodulin), glycocalyx degradation, loss of endothelial barrier function and EC procoagulable state (increased tissue factor expression). Supplementation of the heparan sulfate mimetic fucoidan restores the endothelial glycocalyx and barrier function and reverses the endothelial procoagulable state.

Supplementary figures

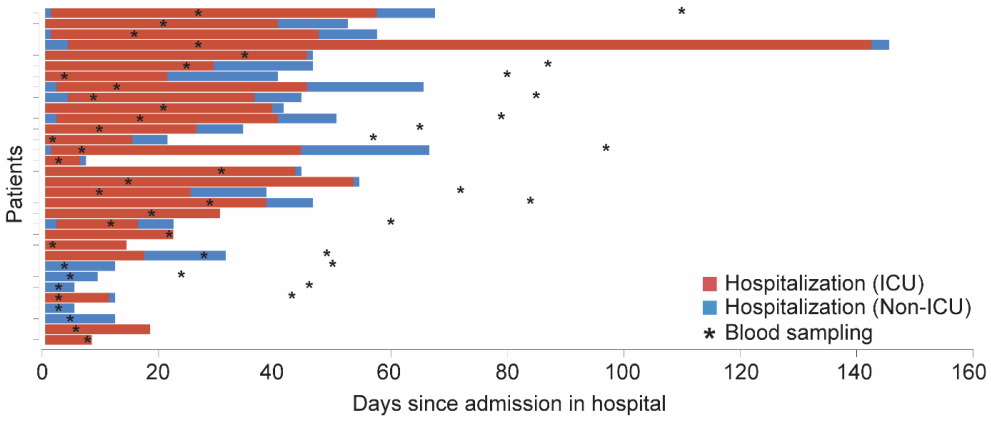

Supplementary figure S1 Patient's hospitalization timelines and blood sampling dates. For each included patient, hospitalization on non-ICU (blue bar), and on ICU (red bar) are indicated, aligned to the day of admission. * represent blood sampling date. For some of the patients, blood samples were collected during the whole hospitalization (ICU and non-ICU) and recovery state (discharge after 6 weeks).

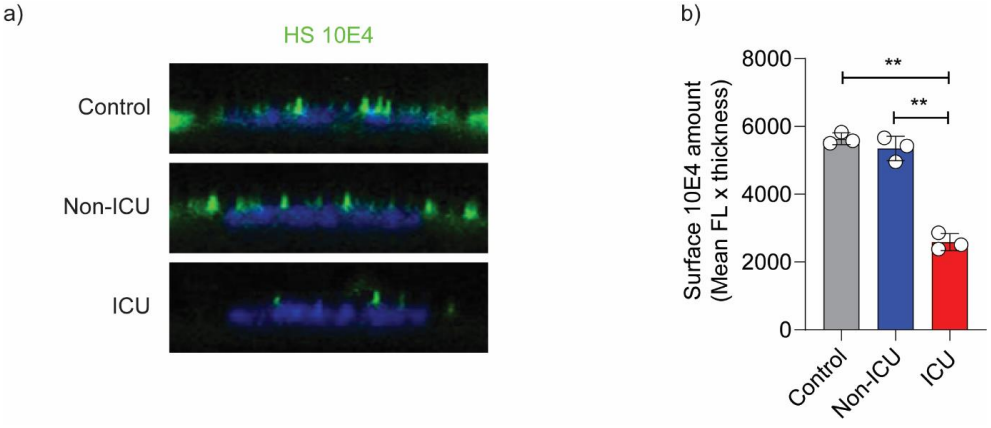

Supplementary figure S2 Loss of heparan sulfate in primary human pulmonary microvascular endothelial cells in presence of COVID-19 ICU serum. a) Representative confocal images of anti-heparan sulfate (HS, 10E4 clone) staining on the surface of primary human pulmonary microvascular endothelial cells (HPMECs) in the presence of 10% pooled- healthy control (n = 12), COVID-19 non-ICU (n = 8) and COVID-19 ICU (n = 26) serum for 24hrs. b) Quantification of HPMECs surface HS (10E4 clone) in the presence of

10% pooled- healthy control, COVID-19 non-ICU and COVID-19 ICU serum for 24hrs, presented as mean fluorescence times thickness of 3 independent experiments. Graphs represent the mean ± SD. One-way ANOVA followed by Tukey's multiple comparisons test were performed; **p<0.01

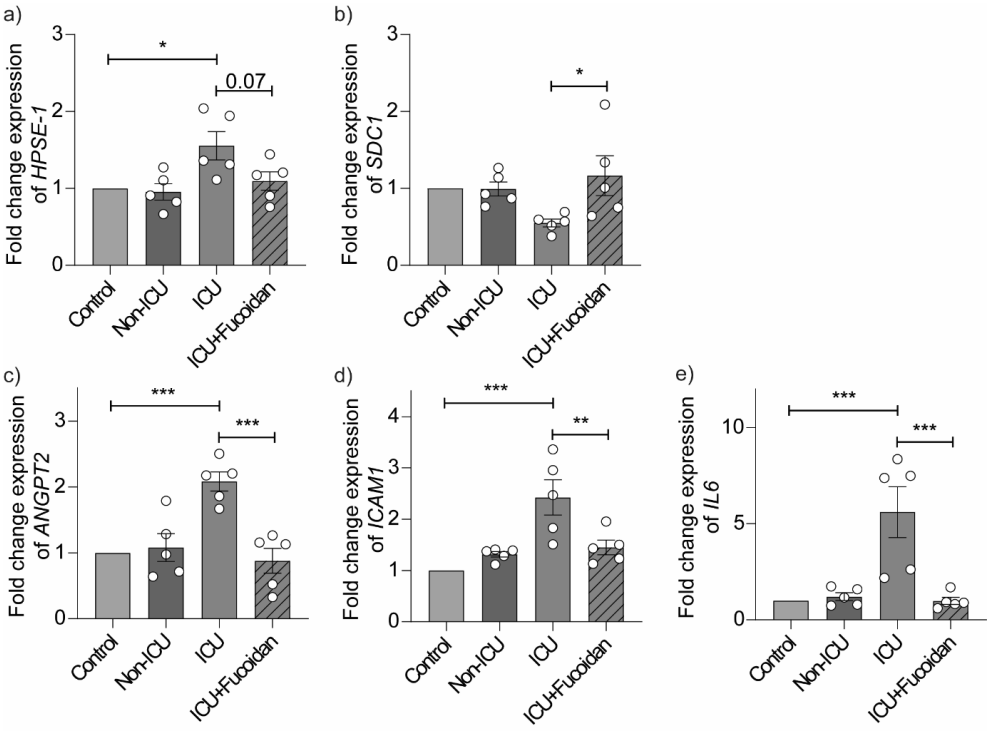

Supplementary figure S3 Fucoidan reduces mRNA expression of endothelial activation related markers. Gene expression data a) heparanase (*HPSE-1*), b) syndecan-1 (*SDC1*), c) *ICAM1*, d) angiopoietin 2 (*ANGPT2*) and e) *IL6* expression in response to 10% pooled-healthy control (n = 12), COVID-19 non-ICU (n = 8) and COVID-19 ICU (n = 26) serum with and without fucoidan (10 µg/mL) for 24hrs, presented as fold change expression normalized to healthy control of 5 independent experiments. Graphs represent the mean ± SEM. One-way ANOVA followed by Tukey's multiple comparisons test were performed; *p<0.05, **p<0.01, ***p<0.001

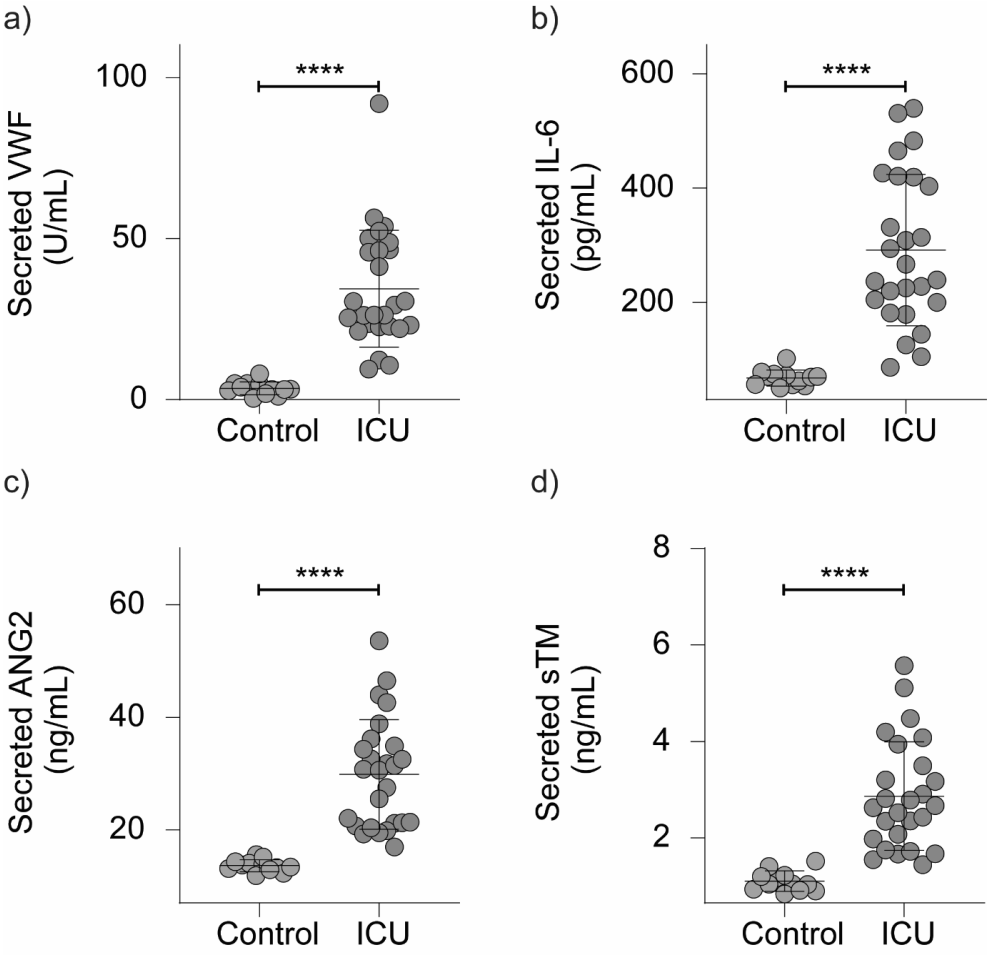

Supplementary figure S4 Comparison of endothelial dysfunction and glycocalyx shedding related markers in cell culture supernatants. Levels of a) secreted von Willebrand factor (VWF), b) secreted IL6, c) secreted angiopoietin 2 (ANG2) and d) secreted soluble thrombomodulin (sTM) in cell culture supernatants of primary human pulmonary microvascular endothelial cells (HPMECS) in the presence of serum of healthy controls (grey, n = 12) and COVID-19 ICU patients (red, n = 26). Nonpaired two-tailed Student t test were performed; *p<0.05, **p<0.01, ***p<0.001, ****p<0.0001.

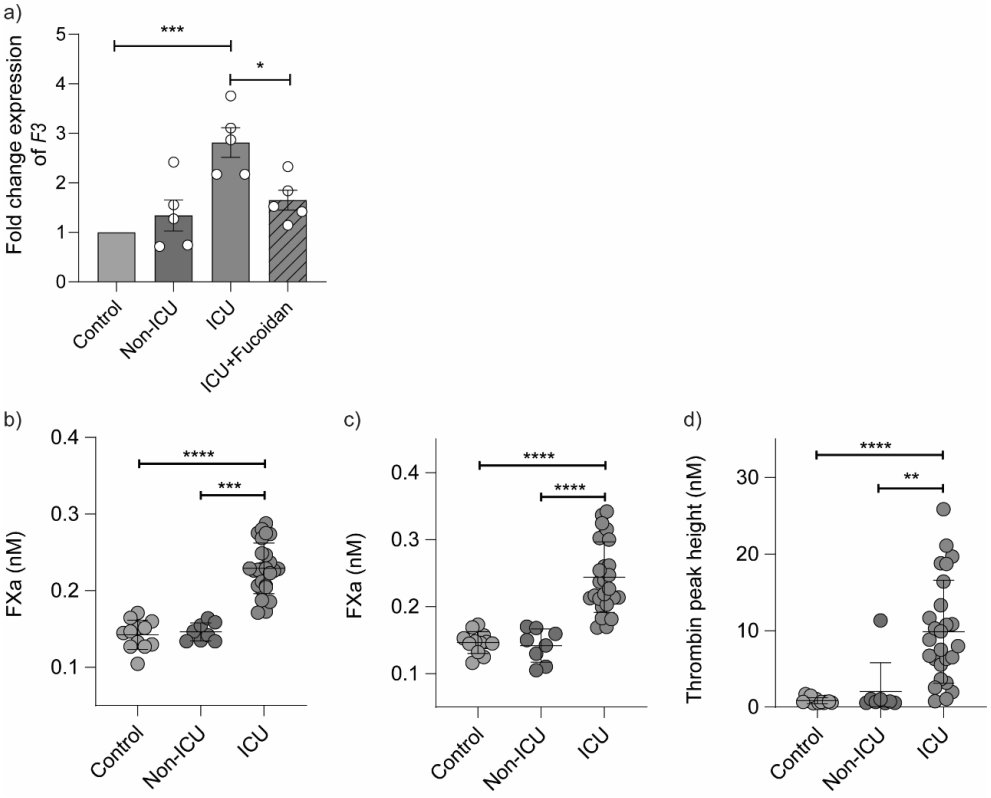

Supplementary figure S5 Serum mediators of COVID-19 patients on ICU promote activation of coagulation on endothelial cells. a) Gene expression of F3 (tissue factor) in response to 10% pooled healthy control (n = 12), COVID-19 non-ICU (n = 8) and COVID-19 ICU (n = 26) serum with and without fucoidan (10 µg/mL) for 24hrs, presented as fold change expression normalized to healthy control of 5 independent experiments. Factor X a (FXa) production (nM) in b) first hour and c) second hour on HPMECs surface in the presence of 10% individual healthy control (n=12), COVID-19 non-ICU (n=8) and COVID-19 ICU (n=26) serum for 24hrs . d) Thrombin generation peak height (nM) measured on HPMECs surface in the presence of 10% individual healthy control (n=12), COVID-19 non-ICU (n=8) and COVID-19 ICU (n=26) serum for 24hrs . One-way ANOVA followed by Tukey's multiple comparisons test were performed; *p<0.05, **p<0.01, ***p<0.001, ****p<0.0001.

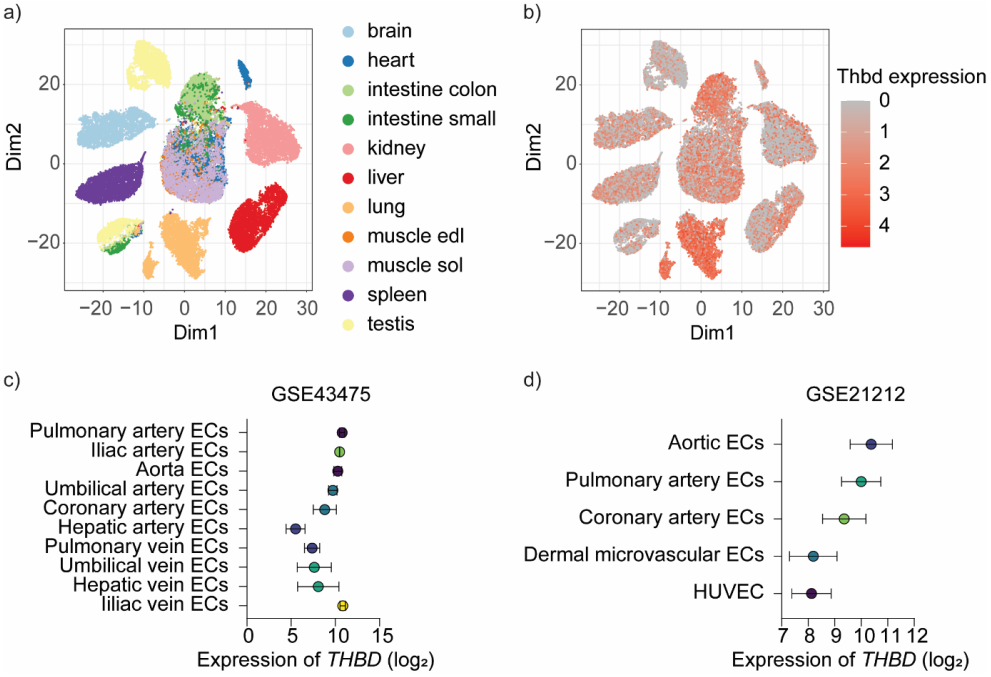

Supplementary figure S6 Thrombomodulin expression levels in different vascular beds. a) tSNE plot revealing gene variation in 11 types of endothelial cells from mice based on EC atlas (https://endotheliomics.shinyapps.io/ec_atlas/). b) Thrombomodulin (*Thbd*) gene expression in 11 types of endothelial cells from mice. *THBD* expression from different human vascular beds based on databases c) GSE43475 and d) GSE21212.

Supplementary table S1. Demographic, clinical, and outcome data of patients in BEAT-COVID cohort

	Hospitalized (n = 32)	ICU (n =26)	Non-ICU (n = 6)	Healthy control (n = 12)
Age - years median (IQR)	61 (57-70)	62 (58-71)	56 (47-65)	60 (60-60)
Male sex - n (%)	26 (81)	21 (81)	5 (83)	8 (75)
BMI - kg/m2 median (IQR)	28 (24-30)	29 (26-30)	25 (20-32)	-
Admission Glasgow Coma Score - points median (IQR)	3 (3-15)	3 (3-15)	15 (15-15)	
Days since hospital admission - median (IQR)	36 (14-47)	43 (22-52)	7 (5-11)	-
Days in ICU - median (IQR)	31 (19-43)	31 (19-43)	-	-
In-hospital mortality - n (%)	7 (21.9)	7 (26.9)	0 (0)	-
Glasgow Coma Score - points median (IQR)	3 (3-11.8)	3 (3-5.8)	15 (15-15)	
SOFA score - median (IQR)	7 (7-11)	7 (7-11)	-	-
LUMC severity score - median (IQR)	12 (9.8-14)	13 (12-14)	3 (1.5-3.8)	-
Comorbidities				
Chronic cardiac disease - n (%)	7 (21.9)	6 (23.1)	1 (16.7)	-
Hypertension - n (%)	8 (25)	7 (26.9)	1 (16.7)	-
Chronic pulmonary disease - n (%)	3 (9.4)	3 (11.5)	0 (0)	-
Asthma - n (%)	6 (18.8)	6 (23.1)	0 (0)	-
Chronic kidney disease - n (%)	1 (3.1)	1 (3.9)	0 (0)	-
Chronic neurological disorder - n (%)	3 (9.4)	2 (7.7)	1 (16.7)	-
Diabetes	13 (40.6)	9 (34.6)	4 (66.7)	-
Smoking history - n (%)	10 (31.3)	10 (38.5)	0 (0)	-
Thromboembolic event - n (%)	4 (12.5)	4 (15.4)	0 (0)	-
Coagulopathy - n (%)	1 (3.1)	1 (3.9)	0 (0)	-
Respiratory function				
Respiratory rate - median (IQR)	26.5 (24-30)	28.5 (25-32)	20.5 (17-23)	-
SpO2 - % median (IQR)	90 (89-92)	89.5 (88-90)	94.5 (94-96)	-
FiO2 - % median (IQR)	60 (41-100)	60 (41-100)	-	-
PaO2/FiO2 ratio - median (IQR)	17 (12.7-20.8)	17 (12.7-20.8)	-	-
Non-invasive ventilation - n (%)	8 (25)	7 (27)	1 (17)*	-
Invasive ventilation - n (%)	17 (53)	16 (62)	1 (17)*	-
Coagulation				
Platelets - 10^9/L median (IQR)	230 (200-302)	2245 (194-309)	253 (223-274)	-
aPTT - seconds median (IQR)	37.5 (33.6-39.9)	37.8 (34.4-40.3)	33.5 (31.5-35.5)	-
PT - seconds median (IQR)	16.1 (14.8-16.8)	15.6 (14.7-16.7)	16.65 (16.6-16.7)	-
INR - median (IQR)	1.2 (1.1-1.2)	1.2 (1.1-1.2)	1.2 (1.2-1.2)	-
D-dimer - mg/L median (IQR)	2.24 (1.03-3.96)	2.24 (1.03-3.96)	-	-
Inflammation markers				
CRP - mg/L median (IQR)	164.4 (58.5-245.1)	185.5 (55.1-255.5)	128.8 (76.6-170.9)	-
Urea - mmol/L median (IQR)	13.4 (5.9-16.8)	15.2 (11.5-17.1)	5 (4.5-5.2)	-

* This patient was first in ICU when treated with non-invasive or invasive ventilation, and stopped ventilation when in non-ICU unit. Blood sampling for this patient was during non-ICU hospitalization.

BMI, body mass index; IQR, interquartile range.

Supplementary table S2. Primer sequences

Gene	Forward sequence	Reverse sequence
GAPDH	CCTGCACCACCAACTGCTTA	GGCCATCCACAGTCTTCTGAG
HPSE	TCCTGCGTACCTGAGGTTTG	CCATTCCAACCGTAACTTCTCCT
SDC1	CCACCATGAGACCTCAACCC	GCCACTACAGCCGTATTCTCC
ICAM1	GTATGAACTGAGCAATGTGCAAG	GTTCCACCCGTTCTGGAGTC
ANGPT2	CTCGAATACGATGACTCGGTG	TCATTAGCCACTGAGTGTTGTTT
IL6	GGTACATCCTCGACGGCATCT	GTGCCTCTTTGCTGCTTTCAC
F3 (TF)	CCCAAACCCGTCAATCAAGTC	CCAAGTACGTCTGCTTCACAT